Gene 951 (2025) 149388

Contents lists available at ScienceDirect

Gene

journal homepage: www.elsevier.com/locate/gene

A novel *de novo GFAP* variant causes a juvenile-onset Alexander disease with bilateral vocal cord paralysis

Muhammad Abrar Yousaf [a,1], Arianna Scartezzini [b,1], Chiara Colombo [b], Tiziana Bachetti [c], Elisa Sarto [d], Daniela Di Bella [d], Pamela Lorenzi [a], Michele Tinazzi [b], Gian Maria Fabrizi [b], Gaetano Vattemi [b,*], Anna Savoia [e]

[a] Department of Neurosciences, Biomedicine and Movement Sciences, University of Verona, Verona, Italy
[b] Department of Neurosciences, Biomedicine and Movement Sciences, Section of Clinical Neurology, University of Verona, Verona, Italy
[c] IRCCS Ospedale Policlinico San Martino, Genova, Italy
[d] Unit of Medical Genetics and Neurogenetics, Fondazione IRCCS Istituto Neurologico Carlo Besta, Milan, Italy
[e] Department of Engineering for Innovation Medicine, University of Verona, Verona, Italy

ARTICLE INFO

Keywords:
Alexander disease
glial fibrillary acidic protein (GFAP)
Mutation
Juvenile onset
Leukodystrophy

ABSTRACT

Alexander disease (AxD), an autosomal dominant leukodystrophy, is caused by mutations in the *GFAP*, the gene encoding glial fibrillary acidic protein (GFAP). The disease, classified by age of onset into infantile, juvenile, and adult forms, is characterized by white matter degeneration and astrocytic inclusions called Rosenthal fibers. A patient underwent clinical, radiological, and molecular analyses to confirm a suspected diagnosis of AxD. The functional effect of the variant identified was tested using computational tools and in HeLa and astrocytoma cell lines. We report a case of juvenile AxD that clinically developed acute respiratory distress due to bilateral vocal cord paralysis. Brain and spinal cord MRI revealed the typical findings of the disease, including bulbospinal atrophy and T2-weighted hyperintensities in the frontal periventricular white matter. Molecular genetic testing identified a novel *de novo* c.713 T > G (p.I238S) variant of *GFAP*. *In silico* analyses revealed that the variant at evolutionarily conserved residue likely affects protein function. *In vitro* assays confirmed its pathogenic effect, showing that p.I238S protein expression significantly associates with aggregate formation in cellular models. Extending the clinical and molecular characterization of new cases of AxD is an important achievement to better characterize the disease.

1. Introduction

The human *GFAP* gene, located on chromosome 17q21.31, encodes the 50-kDa glial fibrillary acidic protein (GFAP), one of the major class III intermediate filament proteins of mature astrocytes. Mutations in *GFAP* are the only known cause of Alexander disease (AxD), a rare and progressive autosomal dominant leukodystrophy (OMIM #203450) (Messing, 2018; Messing and Brenner, 2020). Three clinical subtypes can be distinguished according to the age at onset: infantile (birth to 2 years), juvenile (2 to 14 years), and adult (older than 14 years) (Li et al., 2005). Typical MRI findings include marked atrophy of the brainstem and cervical cord with T2 hyperintensities in the periventricular white matter (Paprocka et al., 2024). The infantile variant is characterized by a predominant involvement of the frontal white matter and basal ganglia, often associated with edema and contrast enhancement affecting both gray and white matter structures, including the periventricular rim, ventricular lining, thalamus, and brainstem (van der Knaap et al., 2001). In contrast, the juvenile-adult form is primarily associated with brainstem and cervical atrophy (Farina et al., 2008).

A broad spectrum of *GFAP* mutations, including nucleotide substitutions, small insertions, and deletions, have been associated with AxD; most mutations arise *de novo*, although inherited variants have also

Abbreviations: GFAP, glial fibrillary acidic protein; OMIM, online mendelian inheritance in man; MRI, magnetic resonance imaging; AxD, Alexander disease; NGS, next-generation sequencing; DMEM, Dulbecco's modified eagle medium; GFP, green fluorescent protein; WT, wild-type; DSD-PAGE, sodium dodecyl sulfate–polyacrylamide gel electrophoresis; PBS, phosphate-buffered saline; DAPI, 4′,6-diamidino-2-phenylindole; HT, head trauma; ICU, intensive care unit.

* Corresponding author at: Section of Clinical Neurology, Department of Neurological and Movement Sciences, Piazzale L.A. Scuro 10, 37134 Verona, Italy.
E-mail address: gaetano.vattemi@univr.it (G. Vattemi).

[1] The authors contributed equally.

https://doi.org/10.1016/j.gene.2025.149388
Received 16 December 2024; Received in revised form 24 February 2025; Accepted 2 March 2025
Available online 3 March 2025

been reported, particularly in adult-onset AxD, where penetrance may be more variable (Grossi et al., 2024; Messing, 2018; Messing and Brenner, 2020). All *GFAP* variants lead to the formation of cytoplasmic protein aggregates within astrocytes known as Rosenthal fibers, the pathologic hallmark of the disease. The presence of Rosenthal fibers hinders cytoskeletal organization and impairs the survival and function of astrocytes, ultimately leading to demyelination (Messing, 2018; Messing and Brenner, 2020).

Here, we report a novel missense *GFAP* variant in a patient who developed a bilateral vocal cord paralysis and provide functional data supporting the pathogenic effect of this mutation.

2. Materials and Methods

2.1. Genetic analysis

Genomic DNA of the proband and his parents was isolated from peripheral blood samples and analyzed using the Agilent-QXT method on Illumina MiSeq NGS sequencer for the nine exons and corresponding exon–intron boundaries of the *GFAP* gene. The identified variant was confirmed by Sanger sequencing. Nucleotide numbering reflects the *GFAP* cDNA with + 1 corresponding to the A of the ATG translation initiation codon in the reference sequence (RefSeq NM_002055.5).

The amino acid sequences of the GFAP protein from human and different species across various taxonomic groups were retrieved from the UniProt database (Bateman, 2019). A multiple sequence alignment analysis was conducted using the Clustal Omega tool (Sievers and Higgins, 2018).

The functional effects of the *GFAP* missense variant were assessed using the SIFT (https://sift.bii.a-star.edu.sg/) (Ng and Henikoff, 2003) and PolyPhen-2 (https://genetics.bwh.harvard.edu/pph2/) (Adzhubei et al., 2010) tools. Mutation Taster (https://www.mutationtaster.org/) (Schwarz et al., 2014), PhD-SNP^{g} (https://snps.biofold.org/phd-snpg/) (Capriotti and Fariselli, 2017) and REVEL (https://sites.google.com/site/revelgenomics/) (Hopkins et al., 2023) tools predicted the association of the variant with the disease. Phosphorylation on serine was predicted using NetPhos 3.1 (https://services.healthtech.dtu.dk/services/NetPhos-3.1/) (Blom et al., 1999), with scores above 0.5 indicating likely phosphorylation.

The study was conducted in accordance with the guidelines in the Declaration of Helsinki. The patient was informed on the intention to publish the case report and gave their written consent.

2.2. Cell culture and transfection

HeLa cells and the human astrocytoma cell line U251-MG were cultured in Dulbecco's modified Eagle's Medium (DMEM) and Roswell Park Memorial Institute 1640 (RPMI 1640) media, respectively. Each medium was supplemented with 10 % fetal bovine serum, 1 % L-glutamine, and 1 % penicillin/streptomycin antibiotics. Cultures were maintained in a humidified atmosphere containing 5 % CO_2 at 37 °C.

The wildtype (WT) GFAP plasmid tagged with green fluorescent protein (GFP) (pcDNA3.1-GFAP-GFP) was used as template to generate the c.713 T > G (p.I238S) variant using the QuikChange site-directed mutagenesis kit. The WT and c.715C > T (p.R239C) control plasmids were obtained as previously described (Bachetti et al., 2008).

For transient transfections, 1×10^6 cells were seeded in 60 mm dishes. Upon reaching 70–80 % confluency, cells were transfected with 5 μg of the WT and mutant forms (p.I238S and p.R239C) of GFAP plasmids using Lipofectamine 3000 Transfection Reagent (Invitrogen), according to the manufacturer's protocol.

2.3. SDS-PAGE and immunoblot analysis

Forty-eight hours after transfection, the cells were lysed in RIPA buffer (supplemented with a protease inhibitor cocktail), sonicated and clarified by centrifugation. The protein concentration in the supernatant was determined using a Coomassie (Bradford) protein assay kit (Thermo Fisher Scientific). Denatured proteins were loaded on 10 % polyacrylamide gel, transferred to nitrocellulose membrane, and probed with anti-GFP (chicken) polyclonal primary antibody (1:3000; Rockland, 600–901-B12), followed by goat anti-chicken IgY horseradish peroxidase-conjugated antibody (1:10,000; Invitrogen, PA1-28798). Bands were visualized with SuperSignal™ West Pico PLUS substrate using the Azure c300 system. Anti-GAPDH (rabbit) primary antibody (1:100,000; ABclonal, AC036) and goat anti-rabbit IgG secondary antibody (1:10,000; Invitrogen, A-11011) were used as loading controls.

2.4. Fluorescence microscopy

Cells were seeded onto poly-L-lysine-coated glass coverslips. Forty-eight hours after transfection the cells were washed with PBS and fixed in 2 % paraformaldehyde/PBS at room temperature for 30 min. Coverslips were mounted on glass slides using mounting solution with ProLong Gold antifade reagent containing DAPI (Invitrogen). The subcellular distribution of the GFAP protein was observed by Nikon Eclipse 80i epifluorescence microscope, and images were captured with a 100x objective lens. GFP (green) and DAPI (blue) images were analyzed using Fiji-ImageJ software (Schindelin et al., 2012).

3. Results

3.1. Case report

The proband (II-1), a Caucasian man, was born to non-consanguineous parents (I-1 and I-2) without a history of neurologic disease and had a healthy brother (II-2) (Fig. 1A). His motor and mental development in early childhood were normal, as well as his early academic achievement. At 9 years of age, he presented hyporexia and food regurgitation, and later anorexia nervosa was suggested. He had surgery at age 15 to correct severe dorsolumbar scoliosis. At that time, a brain MRI performed to investigate isolated growth hormone deficiency documented abnormalities in the frontal white matter, pineal gland, diencephalon, pons, and medulla with contrast enhancement of some of these structures, suggesting a non-secreting germinoma. Extensive laboratory investigations and cerebral spinal fluid analysis were unremarkable, thus a conservative approach was adopted with one-year imaging and laboratory follow-up. From his twenties, he experienced episodes of dizziness, vertigo and postural imbalance due to vestibular decompensation, and developed mixed sleep apneas documented on polysomnography. At 33 years of age, he started complaining of mild dysphagia and dysphonia which worsened significantly after a minor head trauma (HT) and from which he recovered with speech therapy. Two years later, the patient was admitted to hospital due to another minor HT, after which he developed progressive dysphagia, hoarseness, and dysphonia. Otolaryngological evaluation revealed bilateral vocal cord paralysis in adduction requiring posterior laser cordotomy. While waiting for the procedure he developed acute respiratory distress and transferred to the intensive care unit (ICU) of our Institute for tracheostomy. Neurological examination documented pyramidal signs, cerebellar ataxia and bulbar dysfunction including dysphagia. Brain and spinal cord MRI showed bulbospinal atrophy and T2-weighted hyperintensities in the frontal periventricular white matter (Fig. 1B). Given the clinical and radiological findings of our patient, a diagnosis of AxD was considered and genetic analysis for *GFAP* gene was performed.

3.2. Genetic findings

In the proband (II-1), the molecular analysis identified the heterozygous c.713 T > G (p.I238S) nucleotide substitution in exon 4 of *GFAP* (NM_002055.5). The parental segregation revealed the wild-type *GFAP* sequence, suggesting a *de novo* inheritance pattern for this variant

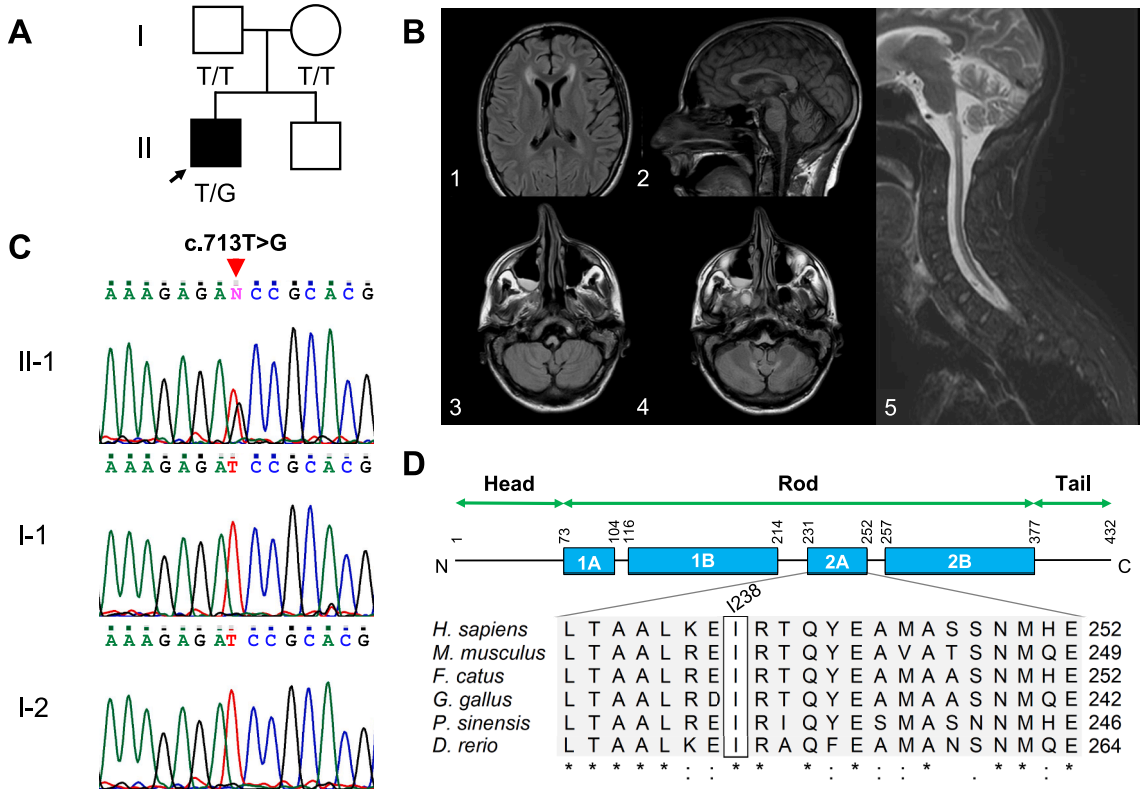

Fig. 1. A: Pedigree enrolled in the study with family member genotypes. The DNA of the younger brother was not analyzed. B: Brain MRI of our patient at the age of 35. Image B1 (axial T2-weighted/FLAIR sequence) shows typical hyperintensities of the periventricular white matter at the frontal horn of the lateral ventricles. Image B2 (sagittal T1-weighted sequence) at midline and images B3 and B4 (axial T2-weighted/FLAIR sequences) at the level of the bulbospinal junction, show severe atrophy of the medulla oblongata. Image B5 (T1-weighted image with fat suppression/STIR) shows atrophy of the medulla oblongata as well as of the cervicodorsal spinal cord. C: Schematic representation of the electropherograms from Sanger sequencing of the *GFAP* gene at position chr17:42.990.704, showing the heterozygous c.713 T > G variant (p.I238S) in the proband (II-1) but not in his parents (I-1 and I-2). D: The structure of GFAP protein comprises three domains: head, rod, and tail. The rod domain is further subdivided into 1A, 1B, 2A, and 2B subdomains, with the residue I238 located specifically in the 2A subdomain. A multiple sequence alignment of the 22 amino acids of the 2A subdomain from different species, including human (*H. sapiens*), mouse (*M. musculus*), cat (*F. catus*), chicken (*G. gallus*), Chinese softshell turtle (*P. sinensis*), and zebrafish (*D. rerio*), is shown. Notably, I238 residue exhibits conservation throughout evolution.

(Fig. 1C & Supplementary file: Fig. 1). Considering almost an equal percentage of the T and G nucleotide reads in the proband and the presence of the WT nucleotide (T) in 100 % of the reads in both parents, it is possible to exclude the presence of mosaicism at least in blood cells (Supplementary file: Fig. 1). The c.713 T > G is not reported in dbSNP or ClinVar databases or scientific literature; it is found in gnomAD at a very low frequency (MAF of 0.0000006196). The p.I238S missense variant affects the 2A subdomain of the rod domain in a region highly conserved. A multiple sequence alignment of the GFAP protein across taxonomic groups highlights the conservation of the I238 residue (Fig. 1D). Substitutions at an amino acid exhibiting greater evolutionary conservation are likely to be pathogenic.

The functional impact of p.I238S was evaluated using *in silico* tools. SIFT predicted the variant to "affect protein function" with a score of 0.00, while PolyPhen2 classified it as "probably damaging" with a score of 0.991. Other tools provided predictions about disease association. Mutation Taster identified the variant as "disease-causing," while PhD-SNPg and REVEL classified it as "pathogenic" with scores of 0.887 and 0.853, respectively. Since c.713 T > G causes the amino acid substitution of isoleucine with serine, we used NetPhos 3.1 to determine the phosphorylation score at the mutant residue. Serine 238 is predicted to generate a site specific for protein kinase A (PKA) with a score of 0.596, which being > 0.5 suggests that the phosphorylation status can be altered in the mutant form of GFAP. This phosphorylation could play a crucial role in the formation of GFAP aggregates in AxD.

Like other intermediate filaments, the assembly of GFAP begins with the parallel alignment of two monomers. This alignment leads to the formation of a two-stranded coiled-coil configuration, which is stabilized by hydrophobic interactions between the α-helices and ionic interactions (Burkhard et al., 2001). Isoleucine, a hydrophobic and nonpolar amino acid, likely participates in this hydrophobic interface, playing a crucial role in maintaining the coiled-coil geometry. Replacing isoleucine with the hydrophilic and polar serine may disrupt the hydrophobic environment, affecting interdimeric interactions and protein folding, potentially leading to misfolded proteins or unstable intermediates. Misfolded proteins often have exposed hydrophobic regions that can lead to aggregation. Furthermore, replacing the large-sized isoleucine with the smaller serine can create a cavity and distort the helical structure, potentially perturbing the dimer-dimer interface.

Altogether, these predictions suggest that residue I238 likely plays a significant role and that its substitution with a serine might lead to functional implications for the GFAP.

3.3. The p.I238S variant caused GFAP aggregation in cellular models

GFAP is an important protein of the intermediate filaments, which are crucial for the cytoskeletal assembly within astrocytes. To investigate whether the GFAP variant alters the intermediate filaments, we expressed the p.I238S GFAP protein in HeLa cells and U251-MG human astrocytoma cells. Initially, we performed Western blot analysis, which shows distinct bands of p.I238S and p.R239C (used as control), confirming their successful transfection and expression in both cell lines (Fig. 2A).

Since previous studies have shown that mutations in GFAP disturb

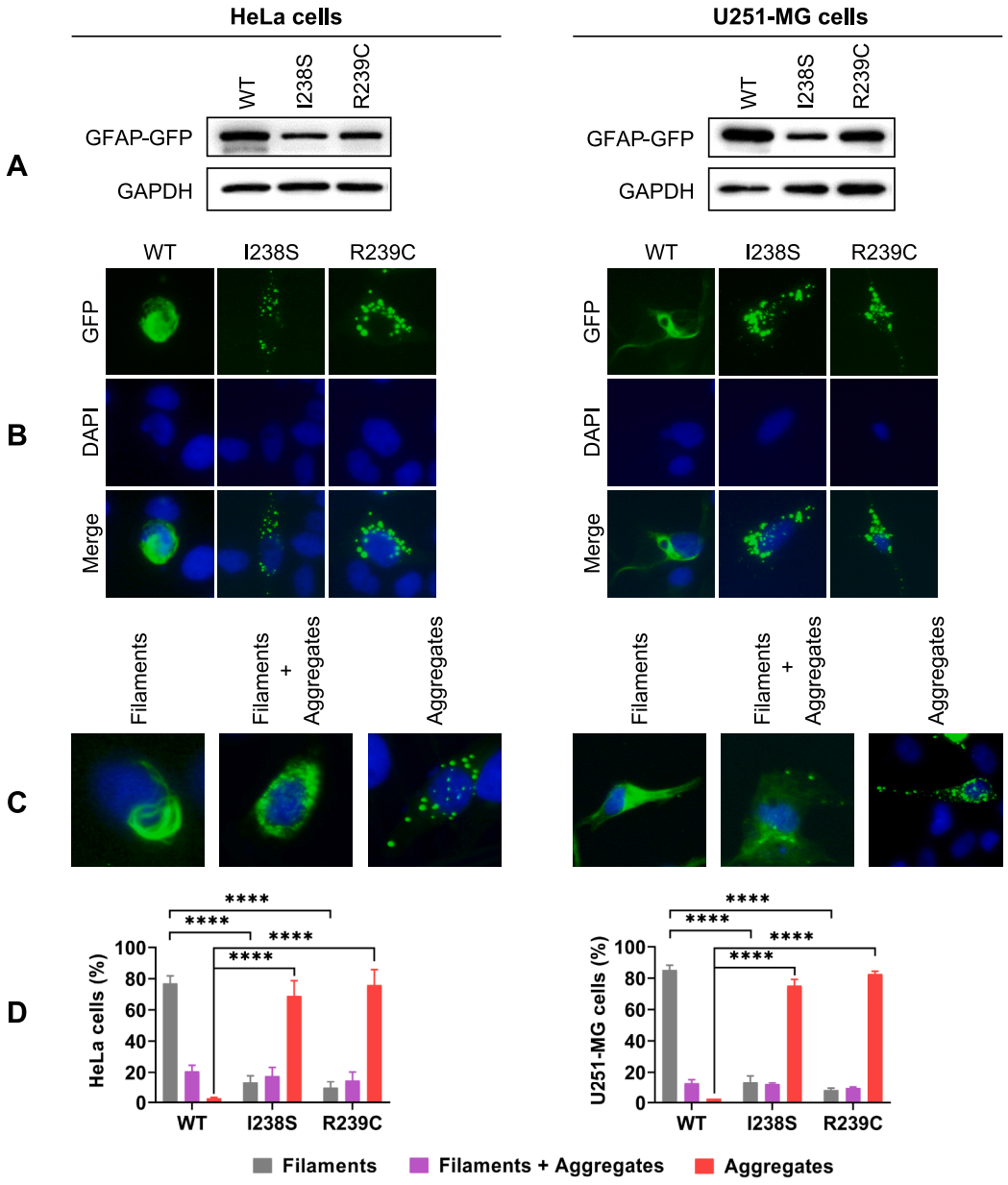

Fig. 2. Exogenous GFAP expression in HeLa and U251-MG human astrocytes cell lines. A: HeLa and U251-MG cells were transfected with plasmids encoding GFP-tagged GFAP (WT and mutants). Western blotting using an anti-GFP antibody shows the expression of exogenous proteins. GAPDH served as a loading control. B: Fluorescence microscopy images of HeLa and U251-MG cells transfected with the WT or mutant forms of GFAP display the protein expression in the cytoplasm. GFAP proteins are in green for the GFP tag (first line), nuclei are stained blue with DAPI (second line), and the merged images are in the third row. In both cell lines, the representative images show that the WT protein predominantly formed filamentous patterns around the nucleus, while the p.I238S and p.R239C mutants mainly exhibited dot-like aggregates. C: Overall, three distinct GFAP patterns were observed in the cytoplasm of both HeLa and U251-MG cells: filamentous assembly, filaments with dot-like aggregates, and only dot-like aggregates. D: Bar graphs showed the percentages of HeLa and U251-MG cells expressing GFAP-GFP WT or mutant constructs, characterized by the three different GFAP patterns. Two-way ANOVA indicated a significant difference between WT and mutant groups (****$p < 0.0001$), with results represented as mean ± standard deviation. In both cell lines, WT GFAP primarily exhibited filamentous patterns, which were significantly higher than in mutants. The novel p.I238S variant and control mutant p.R239C showed significantly higher percentages of dot-like aggregates compared to WT, indicating disease pathology. All experiments were performed in at least three replicates.

the assembly of intermediate filaments (Messing, 2018), we conducted fluorescence analysis in HeLa and U251-MG cell lines transfected with a GFP-tagged GFAP plasmid to determine whether the expression of the mutant proteins is associated with aggregate formation. Most WT GFAP is organized into filaments throughout the cytoplasm (Fig. 2B). Conversely, cells expressing the known p.R239C mutant displayed punctate aggregates, validating the use of our cellular model. The p.I238S mutant predominantly aggregated into clusters as the control mutation, confirming the pathogenic effect of the novel GFAP variant.

Overall, the fluorescence microscopy revealed three distinct patterns of GFAP distribution in the cytoplasm of both transfected cell lines. Some cells displayed a diffuse filament assembly of GFAP, identical to the endogenous intermediate filament network. Other cells showed GFAP in filamentous patterns along with dot-like cytoplasmic aggregates. A third group of cells exhibited only dot-like cytoplasmic aggregates of GFAP (Fig. 2C). Therefore, in the two cellular models we determine the number of cells showing the different distribution patterns. Statistical analysis showed significant differences in the organizational patterns between WT and mutant GFAPs in both cell lines (Fig. 2D). HeLa and U251-MG cells expressing WT protein generally

formed the filamentous organization of GFAP (between 77 % and 85.2 % in the two cell lines), with fewer cells showing mixed patterns of filaments with aggregates (20.5–12.3 %) and very few cells displaying only aggregates (2.6–2.5 %). Cells transfected with the p.I238S variant construct displayed a significantly higher percentage of dot-like GFAP aggregates (68.9 % in HeLa and 75.3 % in U251-MG cells) compared to WT. These aggregates were either large and distributed around the nucleus or small and spread throughout the cytoplasm. The results were comparable to the aggregate formation seen in p.R239C (75.8 % in HeLa and 82.7 % in U251-MG cells) U251-MG transfected cells, suggesting the pathogenicity of the novel p.I238S variant. Furthermore, the percentage of cells exhibiting filamentous patterns or coexistence of filaments and aggregates was comparable among mutants in both cell lines (Fig. 2D). Taken together, these data support the pathogenic role of p.I238S in the cellular model.

4. Discussion

In the present study, we report a novel *de novo* mutation in the *GFAP* gene in a patient with a juvenile form of AxD. This mutation causes the substitution of the amino acid isoleucine at codon 238 with a serine (p.I238S). The presence of *de novo* mutations in AxD is relatively common, particularly in the infantile form, as reported in several index cases tested for segregation (Heshmatzad et al., 2021).

Several *in silico* tools, including evolutionary conservation, classified the variant as pathogenic. Moreover, serine 238 is predicted to be phosphorylated, suggesting that the GFAP activity, stability and interaction with other partners could be affected even by an altered phosphorylation status. A previous study found elevated phosphorylation levels in AxD patients. An added phosphate enhances GFAP proteolysis, producing breakdown products that promote GFAP aggregation. Both phosphorylated GFAP and the proteolytic enzyme have been found to accumulate in astrocyte aggregates (Battaglia et al., 2019). Altogether the predictions suggest a deleterious effect of this variant on the function of the protein.

We functionally validate this hypothesis by expressing the GFAP mutant protein in HeLa and U251-MG astrocytoma cell lines. We found that the exogenous p.I238S protein of GFAP is expressed and predominantly localized within cytoplasmic aggregates mainly distributed around the nucleus. The pattern is the same as that we observe in cells expressing the known p.R239C mutation and other pathogenic variants reported in the literature (Heaven et al., 2019; Hsiao et al., 2005; Perng et al., 2006).

Although p.I238S is enlisted in genomic population datasets (gnomAD) because it is identified in one allele, at least to our knowledge, it has never been associated with the disease, suggesting that it is a novel mutation of GFAP.

The patient was diagnosed as juvenile AxD based on the age of onset, clinical characteristics, and radiological findings. He presented with bulbar symptoms that improved spontaneously or after rehabilitation. Partial or complete remission has been reported in juvenile AxD representing one of the most common factor leading to misdiagnosis; indeed the patient had initially a diagnosis of anorexia nervosa (Namekawa et al., 2012; Wang et al., 2011). MRI is one of the most useful diagnostic tools, as the juvenile and adult form of the disease characteristically reveals atrophy of the bulbar region and upper cervical spinal cord associated with T2-weighted hyperintensities of the frontal periventricular white matter. Persistent contrast enhancement involving the brainstem before bulbar atrophy has been also observed in AxD, mimicking an inflammatory disease or neoplastic lesion as occurred in our patient who received a germinoma misdiagnosis at the age of 15 years (Farina et al., 2008; Yoshida et al., 2021).

The patient is of clinical interest mainly for the first symptom that led to neurological evaluation, the bilateral vocal cord paralysis causing acute respiratory failure. Despite mild and transitory dysphonia has already been described in AxD patients, to date, only one case of acute vocal cord abductor paralysis during sleep requiring tracheostomy has been reported (Hida et al., 2012). The pathogenesis of vocal cord paralysis in AxD is not fully understood but may be due to degeneration of the nucleus ambiguous, the same mechanism underlying the sleep disorders in multiple system atrophy (Isozaki et al., 1996). It is also plausible that brainstem respiratory control centers could be affected in the disease and contribute to respiratory dysfunctions. Indeed, sleep disturbance is a common finding in patients with AxD (Ishikawa et al., 2010).

The acute worsening of symptoms associated with a minor HT is consistent with recent literature (Benzoni et al., 2020). The patient experienced two traumatic brain injuries, with the second one followed by a severe progression leading to permanent tracheostomy and percutaneous endoscopic gastrostomy within two months. Microstructural changes in the corticospinal tract due to posttraumatic swollen astrocytes and reactive gliosis might underlie the neuropathologic mechanisms for clinical deterioration after HT in the disease. The timing and the severity of clinical worsening are variable, up to 10 years, and often lead to a fatal outcome (Benzoni et al., 2020; Goerttler et al., 2022).

In conclusion, we characterized a patient with atypical clinical features of a juvenile form of AxD carrying a novel missense variant of GFAP, which can finally be classified as pathogenic because the expression of the relative mutant protein leads to the formation of dot-like aggregates *in vitro*.

Author Contributions.

MAY, ASc, ES, DDB and PL performed the research and analyzed the data; TB, GV and ASa designed the research study; ASc, CC, MT, GMF and GV enrolled the patient and analyzed clinical data; MAY, ASc, CC, GV, ASa wrote the paper. All the authors read, revised and approved the final manuscript.

Research data for this article.

All data has been included in this paper.

CRediT authorship contribution statement

Muhammad Abrar Yousaf: Writing – original draft, Visualization, Software, Methodology, Investigation, Formal analysis, Data curation. **Arianna Scartezzini:** Writing – original draft, Methodology, Investigation, Formal analysis. **Chiara Colombo:** Writing – original draft, Formal analysis. **Tiziana Bachetti:** Investigation, Conceptualization. **Elisa Sarto:** Methodology, Investigation, Formal analysis. **Daniela Di Bella:** Methodology, Investigation, Formal analysis. **Pamela Lorenzi:** Methodology, Investigation, Formal analysis. **Michele Tinazzi:** Investigation, Formal analysis, Data curation. **Gian Maria Fabrizi:** Investigation, Formal analysis, Data curation. **Gaetano Vattemi:** Writing – review & editing, Supervision, Project administration, Methodology, Investigation, Data curation, Conceptualization. **Anna Savoia:** Writing – review & editing, Validation, Supervision, Resources, Project administration, Data curation, Conceptualization.

Declaration of competing interest

The authors declare that they have no known competing financial interests or personal relationships that could have appeared to influence the work reported in this paper.

Acknowledgments

This paper and the research behind were performed as part of the Excellence Project 2023-2027, funded by MUR, of the Department of Neurosciences, Biomedicine and Movement Sciences of the University of Verona. This work was also supported by grants of “Associazione Più Unici che Rari, Odv” (to TB) and IRCCS Ospedale Policlinico San Martino - Genova (Ricerca Corrente U733A to TB).

Appendix A. Supplementary data

Supplementary data to this article can be found online at https://doi.org/10.1016/j.gene.2025.149388.

References

Adzhubei, I.A., Schmidt, S., Peshkin, L., Ramensky, V.E., Gerasimova, A., Bork, P., Kondrashov, A.S., Sunyaev, S.R., 2010. A method and server for predicting damaging missense mutations. Nat. Methods. https://doi.org/10.1038/nmeth0410-248.

Bachetti, T., Caroli, F., Bocca, P., Prigione, I., Balbi, P., Biancheri, R., Filocamo, M., Mariotti, C., Pareyson, D., Ravazzolo, R., Ceccherini, I., 2008. Mild functional effects of a novel GFAP mutant allele identified in a familial case of adult-onset Alexander disease. Eur. J. Hum. Genet. 16, 462–470. https://doi.org/10.1038/sj.ejhg.5201995.

Bateman, A., 2019. UniProt: A worldwide hub of protein knowledge. Nucleic Acids Res. 47, D506–D515. https://doi.org/10.1093/nar/gky1049.

Battaglia, R.A., Beltran, A.S., Delic, S., Dumitru, R., Robinson, J.A., Kabiraj, P., Herring, L.E., Madden, V.J., Ravinder, N., Willems, E., Newman, R.A., Quinlan, R.A., Goldman, J.E., Perng, M.-D., Inagaki, M., Snider, N.T., 2019. Site-specific phosphorylation and caspase cleavage of GFAP are new markers of Alexander disease severity. Elife 8. https://doi.org/10.7554/eLife.47789.

Benzoni, C., Aquino, D., Di Bella, D., Sarto, E., Moscatelli, M., Pareyson, D., Taroni, F., Salsano, E., 2020. Severe worsening of adult-onset Alexander disease after minor head trauma: Report of two patients and review of the literature. J. Clin. Neurosci. 75, 221–223. https://doi.org/10.1016/j.jocn.2020.03.033.

Blom, N., Gammeltoft, S., Brunak, S., 1999. Sequence and structure-based prediction of eukaryotic protein phosphorylation sites. J. Mol. Biol. 294, 1351–1362. https://doi.org/10.1006/jmbi.1999.3310.

Burkhard, P., Stetefeld, J., Strelkov, S.V., 2001. Coiled coils: a highly versatile protein folding motif. Trends Cell Biol. 11, 82–88. https://doi.org/10.1016/S0962-8924(00)01898-5.

Capriotti, E., Fariselli, P., 2017. PhD-SNPg: a webserver and lightweight tool for scoring single nucleotide variants. Nucleic Acids Res. 45, W247–W252. https://doi.org/10.1093/NAR/GKX369.

Farina, L., Pareyson, D., Minati, L., Ceccherini, I., Chiapparini, L., Romano, S., Gambaro, P., Fancellu, R., Savoiardo, M., 2008. Can MR Imaging Diagnose Adult-Onset Alexander Disease? Am. J. Neuroradiol. 29, 1190 LP – 1196. Doi: 10.3174/ajnr.A1060.

Goerttler, T., Zanetti, L., Regoni, M., Egger, K., Kellner, E., 2022. Adult-Onset Alexander Disease : New Causal Sequence Variant in the GFAP. Gene 1–5. https://doi.org/10.1212/NXG.0000000000000681.

Grossi, A., Rosamilia, F., Carestiato, S., Salsano, E., Ceccherini, I., Bachetti, T., 2024. A systematic review and meta-analysis of GFAP gene variants in Alexander disease. Sci. Rep. 14, 24341. https://doi.org/10.1038/s41598-024-75383-4.

Heaven, M.R., Wilson, L., Barnes, S., Brenner, M., 2019. Relative stabilities of wild-type and mutant glial fibrillary acidic protein in patients with Alexander disease. J. Biol. Chem. 294, 15604–15612. https://doi.org/10.1074/jbc.RA119.009777.

Heshmatzad, K., Haghi Panah, M., Tavasoli, A.R., Ashrafi, M.R., Mahdieh, N., Rabbani, B., 2021. GFAP variants leading to infantile Alexander disease: Phenotype and genotype analysis of 135 cases and report of a de novo variant. Clin. Neurol. Neurosurg. 207, 106754. https://doi.org/10.1016/j.clineuro.2021.106754.

Hida, A., Ishiura, H., Arai, N., 2012. Adult-Onset Alexander Disease with an R66Q Mutation in GFAP Presented with Severe Vocal Cord Paralysis during Sleep 259, 2234–2236. https://doi.org/10.1007/s00415-012-6540-4.

Hopkins, J.J., Wakeling, M.N., Johnson, M.B., Flanagan, S.E., Laver, T.W., 2023. REVEL Is Better at Predicting Pathogenicity of Loss-of-Function than Gain-of-Function Variants. Hum. Mutat. 2023, 1–6. https://doi.org/10.1155/2023/8857940.

Hsiao, V.C., Tian, R., Long, H., Der Perng, M., Brenner, M., Quinlan, R.A., Goldman, J.E., 2005. Alexander-disease mutation of GFAP causes filament disorganization and decreased solubility of GFAP. J. Cell Sci. 118, 2057–2065. https://doi.org/10.1242/jcs.02339.

Ishikawa, M., Shimohata, T., Ishihara, T., Nakayama, H., Tomita, M., Nishizawa, M., 2010. Sleep apnea associated with floppy epiglottis in adult-onset Alexander disease: A case report. Mov. Disord. 25, 1098–1100. https://doi.org/10.1002/mds.23042.

Isozaki, E., Naito, A., Horiguchi, S., Kawamura, R., Hayashida, T., Tanabe, H., 1996. Early diagnosis and stage classification of vocal cord abductor paralysis in patients with multiple system atrophy. J. Neurol. Neurosurg. & Psychiatry 60, 399 LP – 402. Doi: 10.1136/jnnp.60.4.399.

Li, R., Johnson, A.B., Salomons, G., Goldman, J.E., Naidu, S., Quinlan, R., Cree, B., Ruyle, S.Z., Banwell, B., D'Hooghe, M., Siebert, J.R., Rolf, C.M., Cox, H., Reddy, A., Gutiérrez-Solana, L.G., Collins, A., Weller, R.O., Messing, A., van der Knaap, M.S., Brenner, M., 2005. Glial fibrillary acidic protein mutations in infantile, juvenile, and adult forms of Alexander disease. Ann. Neurol. 57, 310–326. https://doi.org/10.1002/ana.20406.

Messing, A., 2018. Alexander disease. Handbook of Clinical Neurology. 693–700. https://doi.org/10.1016/B978-0-444-64076-5.00044-2.

Messing, A., Brenner, M., 2020. GFAP at 50. ASN Neuro 12. https://doi.org/10.1177/1759091420949680.

Namekawa, M., Takiyama, Y., Honda, J., 2012. CASE REPORT A novel adult case of juvenile-onset Alexander disease : complete remission of neurological symptoms for over 12 years , despite insidiously progressive cervicomedullary atrophy. Neurol. Sci. 33, 1389–1392. https://doi.org/10.1007/s10072-011-0902-z.

Ng, P.C., Henikoff, S., 2003. SIFT: predicting amino acid changes that affect protein function. Nucleic Acids Res. 31, 3812–3814. https://doi.org/10.1093/NAR/GKG509.

Paprocka, J., Nowak, M., Machnikowska-Sokołowska, M., Rutkowska, K., Płoski, R., 2024. Leukodystrophy with Macrocephaly, Refractory Epilepsy, and Severe Hyponatremia—The Neonatal Type of Alexander Disease. Genes (basel). 15, 350. https://doi.org/10.3390/genes15030350.

Perng, M.D., Su, M., Wen, S.F., Li, R., Gibbon, T., Prescott, A.R., Brenner, M., Quinlan, R. A., 2006. The Alexander Disease – Causing Glial Fibrillary Acidic Protein Mutant , R416W , Accumulates into Rosenthal Fibers by a Pathway That Involves Filament Aggregation and the Association of a B-Crystallin and HSP27. Am. J. Hum. Genet. 79, 197–213.

Schindelin, J., Arganda-Carreras, I., Frise, E., Kaynig, V., Longair, M., Pietzsch, T., Preibisch, S., Rueden, C., Saalfeld, S., Schmid, B., Tinevez, J.-Y., White, D.J., Hartenstein, V., Eliceiri, K., Tomancak, P., Cardona, A., 2012. Fiji: an open-source platform for biological-image analysis. Nat. Methods 9, 676–682. https://doi.org/10.1038/nmeth.2019.

Schwarz, J.M., Cooper, D.N., Schuelke, M., Seelow, D., 2014. MutationTaster2: mutation prediction for the deep-sequencing age. Nat. Methods 11, 361–362. https://doi.org/10.1038/nmeth.2890.

Sievers, F., Higgins, D.G., 2018. Clustal Omega for making accurate alignments of many protein sequences. Protein Sci. 27, 135–145. https://doi.org/10.1002/pro.3290.

van der Knaap, M.S., Naidu, S., Breiter, S.N., Blaser, S., Stroink, H., Springer, S., Begeer, J.C., van Coster, R., Barth, P.G., Thomas, N.H., Valk, J., Powers, J.M., 2001. Alexander disease: diagnosis with MR imaging. AJNR. Am. J. Neuroradiol. 22, 541–552.

Wang, J., Morizono, H., Gordon, E., Hartka, T., Fleming, J., Gill, D., 2011. GFAP Mutations , Age at Onset , and Clinical Subtypes in Alexander Disease 77, 1287–1294.

Yoshida, T., Mizuta, I., Yasuda, R., Mizuno, T., 2021. Clinical and Radiological Characteristics of Older- - Onset Alexander Disease 28, 3760–3767. https://doi.org/10.1111/ene.15017.